Extension rates, crustal melting, and core complex dynamics

P.F. Rey[1*], C. Teyssier[2], and D.L. Whitney[2]
[1]Earthbyte Research Group, School of Geosciences, University of Sydney, Sydney, NSW 2006, Australia
[2]Department of Geology and Geophysics, University of Minnesota, Minneapolis, Minnesota 55455, USA

ABSTRACT

Two-dimensional thermomechanical experiments reveal that the crystallization versus exhumation histories of migmatite cores in metamorphic core complexes give insights into the driving far-field extensional strain rates. At high strain rates, migmatite cores crystallize and cool along a hot geothermal gradient (35–65 °C km^{-1}) after the bulk of their exhumation. At low strain rates, migmatite cores crystallize at higher pressure before the bulk of their exhumation, which is accommodated by solid-state deformation along a cooler geothermal gradient (20–35 °C km^{-1}). In the cases of boundary-driven extension, space is provided for the domes, and therefore the buoyancy of migmatite cores contributes little to the dynamics of metamorphic core complexes. The presence of melt favors heterogeneous bulk pure shear of the dome, as opposed to bulk simple shear, which dominates in melt-absent experiments. The position of migmatite cores in their domes reveals the initial dip direction of detachment faults. The migmatitic Shuswap core complex (British Columbia, Canada) and the Ruby–East Humboldt Range (Nevada, United States) possibly exemplified metamorphic core complexes driven by faster and slower extension, respectively.

INTRODUCTION

Migmatite-cored metamorphic core complexes are common crustal-scale features that develop when thick, partially molten continental crust is exhumed beneath low-angle normal faults (detachments) by extension. They offer an opportunity to study deep crustal processes, contribute to the thermal and mechanical reequilibration of orogenic crust, and, as we show here, record the kinematic boundary conditions prevailing during the final stages of orogeny.

Physical and numerical experiments have shown that strain localization is essential to metamorphic core complexes (Buck, 1993; Lavier et al., 1999; Koyi and Skelton, 2001; Dyksterhuis et al., 2007; Gessner et al., 2007; Brun et al., 1994; Tirel et al., 2004; Wijns et al., 2005, Regenauer-Lieb et al., 2006). Upon extension, localized thinning of the upper crust is isostatically compensated by the flow of ductile lower crust into the metamorphic core complex (Block and Royden, 1990; Wdowinski and Axen, 1992), requiring a low-viscosity lower crust (Brun et al., 1994; Wijns et al., 2005). The viscosity of partially melted rocks decreases dramatically with increasing melt fraction (Richet and Bottinga, 1995; Scaillet et al., 1996; Baker, 1998) and, in the common case of fluid-absent partial melting, density also decreases (Clemens and Droop, 1998). As most fluid-absent melting reactions have positive slope in pressure-temperature space, extension-induced decompression could be important in the structural and thermal development of migmatite-cored metamorphic core complexes (Teyssier and Whitney, 2002; Whitney et al., 2004). Very few studies have investigated the role of partial melting in the development of metamorphic core complexes (Tirel et al., 2004, 2008) and none includes temperature-dependent melt fraction and/or melt fraction–dependent viscosity and density.

We examine the thermal and mechanical evolution of metamorphic core complexes via a series of two-dimensional numerical experiments in which the impacts of partial melting on temperature, density, and viscosity are accounted for. Because heat advection competes with the conductive cooling of the thinning crust, the role of extensional strain rates is also considered. We compare numerical experiments results with natural examples of migmatite-cored metamorphic core complexes and show that the position of the migmatite core within domes, the crystallization depth, the shape of particle flow paths (kinematics and finite strain), and pressure-temperature-time (*P-T-t*) paths are critically dependent on extensional strain rates and melt fraction.

NUMERICAL EXPERIMENTS, CODE AND MODEL SETUP

We use Ellipsis, a Lagrangian integration point finite-element code, to solve the governing equations of momentum, mass, and energy in incompressible flow (Moresi et al., 2003). Figure 1 describes the geometry and thermomechanical state of our reference model (see the GSA Data Repository[1] for details). In contrast to previous studies (Brun et al., 1994; Brun, 1999; Tirel et al., 2004, 2008; Wijns et al., 2005; Gessner et al., 2007), the upper and lower crust in our models have the same rheology and density structures, so the depth of the brittle-ductile transition evolves with strain rate and temperature.

A melt function was implemented in Ellipsis to account for the thermal and mechanical effects of partial melting (O'Neill et al., 2006). The solidus and liquidus are adjusted to obtain a peak melt fraction of 35% at the Moho (Fig. 1). The density of the partially melted region decreases linearly by 13% between the solidus and the liquidus (Clemens and Droop, 1998), whereas the viscosity decreases linearly by three orders of magnitude when the melt fraction increases from 15% to 30%. Rosenberg and Handy (2005) showed that significant weakening occurs at 7% melt fraction. In our experiments, the melt fraction increases up to 30% over a few kilometers. Consequently, the results are not affected by shifting this critical melt fraction down to 2%–12%. In the models, there is no segregation of the melt from its source, a reasonable approximation for many migmatite-cored metamorphic core complexes in which melt and solid fractions move en masse (Teyssier and Whitney, 2002; Whitney et al., 2004).

Moving boundary conditions are imposed at both lateral ends of the model. We have tested a range of initial strain rates between 6×10^{-15} s^{-1} and 2×10^{-16} s^{-1} (i.e., 25.5 mm/yr to 0.85 mm/yr at both sides). These strain rates are achieved for the first increment of deformation and decrease as extension proceeds. Because deformation is strongly localized around the detachment fault, much higher strain rates are achieved around the metamorphic core complex.

METAMORPHIC CORE COMPLEX GEOMETRY, TEMPERATURE, AND PARTIAL MELT DISTRIBUTIONS

Figure 2 shows models deformed at relatively slow (2×10^{-16} s^{-1}) and fast (2×10^{-15} s^{-1}) extension rates. In many dozens of trials with variations in physical and numerical parameters, modeling results are robust with respect to geometry and *P-T-t* evolution. Melt-absent experiments (Figs. 2A and 2B) illustrate the importance of extension rate. Fast extension promotes significant heat advection (relief of isotherms, Fig. 2B) and internal deformation of material in the upwelling region, resulting in a wider metamorphic core complex. This latter result seems at odds with results from physical experiments, which suggest that fast extension leads to distributed surface extension (Brun et al., 1994; Brun, 1999). This discrepancy is likely

*E-mail: p.rey@usyd.edu.au.

[1]GSA Data Repository item 2009099, details of modeling procedures and parameters, is available online at www.geosociety.org/pubs/ft2009.htm, or on request from editing@geosociety.org or Documents Secretary, GSA, P.O. Box 9140, Boulder, CO 80301, USA.

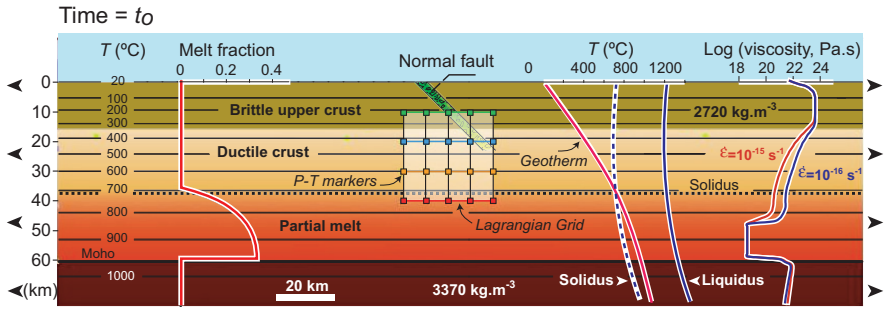

Figure 1. Model geometry, parameters, and boundary conditions, showing solidus and liquidus, geotherm, melt fraction, viscosity, and locations of markers used to track temperature and pressure (*T*, *P*) history, flow paths, and finite strain. Weak prismatic region dipping 45° simulates detachment fault in upper crust. Crust has solidus and liquidus with positive *dP*/*dT* that is representative of fluid-absent partial melting reactions (Clemens and Droop, 1998). Contrasting color between upper and lower crust acts as strain marker.

due to the more realistic visco-plastic stratification in our numerical experiments compared to the shear stress discontinuity at the sand-silicone contact in physical experiments.

With the melt function turned on (Figs. $2C_1$, $2C_2$, $2D_1$, $2D_2$), the core complex broadens slightly (6%–12% wider), whether at slow or fast strain rates. Slow extension with melt (Figs. $2C_1$ and $2C_2$) enhances upward motion of deep crust (Fig. 2A), resulting in larger exhumation of rocks that were once partially molten. Figure $2C_2$ shows an antiform of crystallized partial melt that represents preferential exhumation of deep rocks in the detachment footwall. The solidus at 40 m.y. is relatively flat and located at ~27 km depth. In contrast, fast extension (Figs. $2D_1$ and $2D_2$) produces larger heat advection that also corresponds to upward motion of the partial melt layer. After 4 m.y., the solidus is located at <10 km depth and the partial melt antiform is cored by a region of >30% melt at shallow levels. Despite the symmetry of kinematic boundary conditions, the crystallized migmatite cores are systematically shifted in the domes toward the hanging wall. This shift (cf. Burg et al., 2004) does not exist in experiments (not shown) in which a circular rheological anomaly was used as strain localization agent. We conclude that the shift is linked to the initial dip direction of the planar zone of weakness, which therefore plays an important role in the evolving geometry and the asymmetry of migmatite-cored metamorphic core complexes. In nature, this shift can be used to infer the dip direction of the original detachment fault.

The exhumation magnitude of the solidus, and the crystallization versus exhumation and/or deformation history, are the most fundamental differences between models extending at fast and slow strain rates. Initially at a depth of 37 km, fast extension brings the solidus ~7 km to the surface in a few million years (Fig. $2D_2$). In this case, cooling and crystallization of partially molten crust occurs after the bulk of deformation accommodating the exhumation of the dome, possibly even after extension has stopped, as the solidus recedes downward during cooling of the crust. In contrast, slow extension brings the solidus slowly ~27 km to the surface over a few tens of millions of years (Fig. $2C_2$). In this case, a large volume of migmatite is advected upward through a quasi-static solidus (blue region in Fig. $2C_2$), as rocks are exhumed faster than the solidus. In the latter case, the bulk of deformation accommodating the dome exhumation occurs after crystallization, and partial melting is restricted to $P > 600$ MPa (>~22 km). This contrasted crystallization versus exhumation and/or deformation history suggests that solid-state deformation is dominant in slow extension metamorphic core complexes, whereas weakly deformed domes are expected in fast extension metamorphic core complexes, as crystallization and cooling postdate the bulk of exhumation of the dome. The contrasting crystallization versus exhumation and/or deformation history also suggests that low-pressure partial melting ($P < 400$ MPa, i.e., <~15 km) requires fast extensional strain rates, whereas melts restricted to medium to high pressure ($P > 600$ MPa) are prevalent in slow extension metamorphic core complexes.

To test the role of buoyancy in the upward flow of the low-viscosity layer, we ran experiments in which melting was not accompanied with density decrease. These experiments confirm that, as long as space for metamorphic core complexes is provided by boundary-driven extension, the buoyancy force is secondary to strain rate (Brun et al., 1994; Tirel et al., 2004, 2008; Wijns et al., 2005; Gessner et al., 2007). In a system driven by far-field horizontal extension, upward flow in metamorphic core complexes is determined mainly by a dynamic feedback between extension of the upper crust and the necessity for the low-viscosity lower crust to fill the zone of exten-

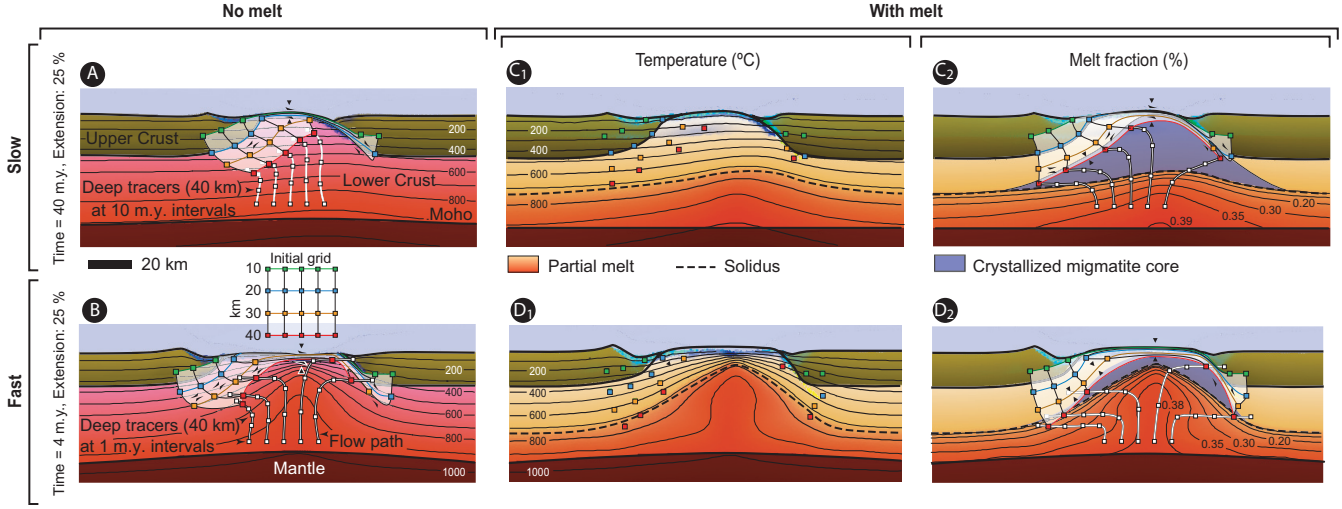

Figure 2. All models have recorded 25% extension following 40 m.y. of extension at strain rate of 2×10^{-16} s^{-1} (A, C) and 4 m.y. of extension at strain rate of 2×10^{-15} s^{-1} (B, D). A, B: Models with melt function turned off, and (C_1, D_1) models with melt function turned on contoured for temperature, and melt fraction (C_2, D_2). Flow paths of deeper grid nodes are shown as thick white lines.

sion efficiently (Wdowinski and Axen, 1992); isostasy rather than buoyancy drives exhumation. Contrasting results can be expected when volume forces, due to lateral variation in gravitational energy, drive extension. In such a case, space for metamorphic core complexes is provided by internal redistribution of masses (Rey et al., 2001), in which case the buoyancy of the melted lower crust is of fundamental importance.

FINITE STRAIN, FLOW, AND *P-T-t* PATHS IN METAMORPHIC CORE COMPLEXES

Although various metamorphic core complexes have similar shapes, their internal deformations differ significantly, as seen by contrasted flow paths and finite strains recorded by a passive grid (Fig. 2). In experiments with no melt, the bulk of the metamorphic core complex region is involved in a combination of counterclockwise rotation (dominant in Fig. 2A), top to the left heterogeneous simple shear, and pure shear (dominant in Fig. 2B). Counterclockwise rotation is the consequence of the interplay between asymmetric simple shear and isostasy, which produces a horizontal exhumation gradient (Fig. 2A). The top right corner of the grid is caught in the detachment zone, recording a top-to-the-right shearing. Prominent early upward motions and later minor horizontal motion characterize the flow path of the lowermost grid nodes (Figs. 2A and 2B). In melt-present experiments, the later horizontal motion is more developed and heterogeneous bulk flattening dominates the finite strain of the grid, except in the vicinity of the active segment of the detachment fault, where top to the right simple shear dominates. Away from the active segment of the detachment, there is a strong contrast between the bulk simple shear that dominates the finite strain in melt-absent fast extension experiments, and the bulk pure shear that dominates in slow extension melt-present experiments.

P-T-t paths are very sensitive to strain rate (Fig. 3). At low extensional strain rate (Figs. 3A and 3C), *P-T-t* paths follow decompression and cooling along a geothermal gradient in the range of 20–35 °C km^{-1}, with similar shapes in experiments with or without partial melting. In all experiments, the 20 km marker, located structurally above the detachment fault (i.e., in the hanging wall), records near isobaric heating. This heating is due to the advection of hot material that occurs under the hanging wall. At higher strain rate (Figs. 3B and 3D), most *P-T-t* paths show an episode of near isothermal decompression before an episode of decompression and cooling along a hotter geothermal gradient (35–65 °C km^{-1}). Deep markers have *P-T-t* paths crossing from the kyanite to the sillimanite stability field, whereas shallower markers cross from the kyanite to the andalusite stability field. At high strain rate, and when melt is present, some *P-T-t* paths show a sudden change from near isothermal decompression to near isobaric cooling (Fig. 3D), consistent with the observed change in direction of the rocks' flow paths.

FIELD EXAMPLES OF FAST AND SLOW MIGMATITE-CORED METAMORPHIC CORE COMPLEXES

Metamorphic core complexes in the North American Cordillera share first-order characteristics, but in detail display a wide range of styles that could be linked to the tempo and duration of extensional deformation, as well as the volume of melt involved. The formation of most of the metamorphic core complexes in the northern Cordillera (Nevada, United States, to British Columbia, Canada) involved crustal melting, whereas metamorphic core complexes in Arizona and southern California developed in a solid-state crust and are dominated by a simple shear detachment zone (cf. Fig. 2B). The Ruby–East Humboldt Range migmatite-cored metamorphic core complex in the Basin and Range (Nevada) and the Shuswap migmatite-cored metamorphic core complex in the Canadian Cordillera exemplify some of the contrasting features that develop under different conditions of melt and extension rate. The geometry, *P-T* evolution, and extension and/or exhumation rates of the Shuswap core complex closely match our models of fast extension in the presence of melt. In this migmatite-cored dome, crystallization of leucogranite and migmatite leucosome occurred between 60 and 52 Ma (Vanderhaeghe et al., 1999; Hinchey et al., 2006), followed by rapid cooling through mica ^{40}Ar/^{39}Ar closure temperatures at 49–48 Ma (Teyssier et al., 2005). The migmatite core is shifted toward the eastern detachment (Columbia River), suggesting that this fault zone acted as an east-dipping rolling hinge that separated the cool and thick foreland crust to the east from the partially molten crust in the hinterland (Teyssier et al., 2005). The *P-T-t* path of dome rocks records near-isothermal decompression from 800–1000 MPa to <500 MPa at ~750 °C (Norlander et al., 2002) under partial-melt conditions, indicating that melt crystallized at low pressure (cf. Figs. 2D$_2$ and 3D).

In contrast, the Ruby–East Humboldt Range migmatite-cored metamorphic core complex records a protracted history of extension and exhumation that may have started as early as the Late Cretaceous and continued during the Eocene to the middle to late Oligocene, when the bulk of metamorphic core complex development occurred (e.g., Sullivan and Snoke, 2007; McGrew et al., 2000). Partial melting in the lower crust, synchronous with extension and exhumation, is evidenced by late Eocene and middle Oligocene granitic plutons, dikes, and sills strongly transposed into the extensional mylonitic fabric (Wright and Snoke, 1993). In the migmatite dome, metamorphic assemblages record, from ca. 85 Ma to ca. 55 Ma, a first episode of synchronous partial melting decompression and cooling from >900 MPa and 800 °C to 700 MPa and 650 °C, along a path subparallel to the kyanite-sillimanite transition (McGrew et al., 2000), compatible with slow exhumation and crystallization at depth. From ca. 55 to ca. 40 Ma, decompression developed under near constant temperature from 700 MPa and 650 °C to 300 MPa and 600 °C. According to our experiments, this second episode is compatible with faster exhumation. Between 35

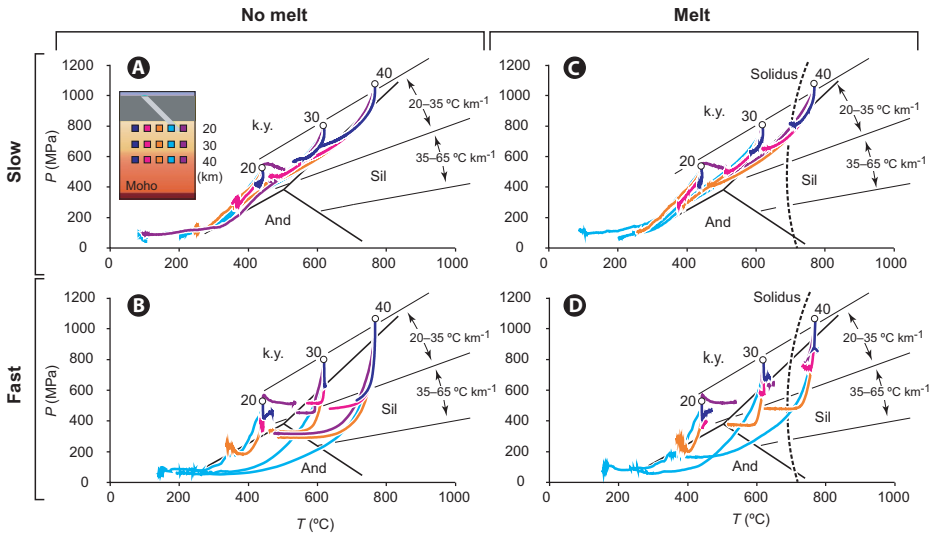

Figure 3. Pressure, temperature, time (*P-T-t*) paths in migmatite-cored metamorphic core complexes for slow and fast strain rates in no-melt models (A, B) and melt-present models (C, D). Color of *P-T-t* paths refers to markers shown in inset in A; their original depths are 20, 30, and 40 km.

and 22 Ma, the third episode of extension, the main metamorphic core complex phase, involved coeval decompression and cooling along a temperature gradient of 40 °C/km (McGrew et al., 2000); according to our experiment, this suggests a slower extension rate.

CONCLUSIONS

Numerical experiments reveal first-order petrological and structural features that can be identified in the field to gain insights into the geometrical and thermal conditions controlling the development of metamorphic core complexes. Major differences exist between two end-member classes of migmatite-cored metamorphic core complexes. Faster migmatite-cored metamorphic core complexes have weakly deformed migmatite cores that record high-temperature decompression and partial melting before cooling along a high geothermal gradient (~35–65 °C km^{-1}). Slower migmatite-cored metamorphic core complexes have migmatite cores that crystallize at high pressure (>600 MPa) before accumulating a large amount of solid-state deformation during coeval decompression and cooling along a cooler thermal gradient (~20–35 °C km^{-1}). A predicted shift of the migmatite core toward the hanging wall is due to strain localization imposed by a detachment fault. The original dip of the detachment fault can be inferred from this shift. The variety in styles observed in metamorphic core complexes can possibly be linked to the tempo and duration of extensional deformation, as well as the volume of melt involved. The Shuswap and Ruby–East Humboldt Range are proposed as possible examples of faster and slower migmatite-cored metamorphic core complexes.

ACKNOWLEDGMENTS

This work benefited from the reviews of R. Weinberg and T.L. Spell and discussions with C. Wijns. It was supported by AuScope–National Collaborative Research Infrastructure Strategy, and Computational Infrastructure for Geodynamics software infrastructure, and a visiting fellowship from the University of Minnesota to Rey. National Science Foundation grant EAR-0409776 supported Teyssier and Whitney's research. Teyssier acknowledges grant 200021-117694 from the Swiss National Science Foundation.

REFERENCES CITED

Baker, D.R., 1998, Granitic melt viscosity and dike formation: Journal of Structural Geology, v. 20, p. 1395–1404, doi: 10.1016/S0191-8141(98)00057-1.

Block, L., and Royden, L., 1990, Core complex geometries and regional scale flow in the lower crust: Tectonics, v. 9, p. 557–567, doi: 10.1029/TC009i004p00557.

Brun, J.-P., 1999, Narrow rifts versus wide rifts: Inferences for the mechanics of rifting from laboratory experiments: Royal Society of London Philosophical Transactions, ser. B, v. 357, p. 695–712.

Brun, J.-P., Soukoutis, D., and Van Den Driessche, J., 1994, Analogue modeling of detachment fault systems and core complex: Geology, v. 22, p. 19–22, doi: 10.1130/0091-7613(1994)022<0319:AMODFS>2.3.CO;2.

Buck, W.R., 1993, Effect of lithospheric thickness on the formation of high- and low-angle normal faults: Geology, v. 21, p. 933–936, doi: 10.1130/0091-7613(1993)021<0933:EOLTOT>2.3.CO;2.

Burg, J.-P., Kaus, B.J.-P., and Podladchikov, Y.Y., 2004, Dome structures in collision orogens: Mechanical investigation of the gravity/compression interplay, *in* Whitney, D.L., et al., eds., Gneiss domes in orogeny: Geological Society of America Special Paper 380, p. 47–66.

Clemens, J.D., and Droop, G.T.R., 1998, Fluids, P-T paths and the fate of anatectic melts in the Earth's crust: Lithos, v. 44, p. 21–36, doi: 10.1016/S0024-4937(98)00020-6.

Dyksterhuis, S., Rey, P., Müller, D., and Moresi. L., 2007, Effect of initial weakness on rift architecture, *in* Karner, G.D., et al., eds., Imaging, mapping and modelling continental lithosphere extension and breakup: Geological Society of London Special Publication 282, p. 443–455.

Gessner, K., Wijns, C., and Moresi, L., 2007, Significance of strain localization in the lower crust for the structural evolution and thermal history of metamorphic core complexes: Tectonics, v. 26, TC2012, doi: 10.1029/2004TC001768.

Hinchey, A.M., Carr, S.D., McNeill, P.D., and Rayner, N., 2006, Paleocene–Eocene high-grade metamorphism, anatexis and deformation in Thor-Odin dome, Monashee complex, southeastern British Columbia: Canadian Journal of Earth Sciences, v. 43, p. 1341–1365, doi: 10.1139/E06-028.

Koyi, H.A., and Skelton, A., 2001, Centrifuge modeling of the evolution of low-angle detachments faults from high-angle normal faults: Journal of Structural Geology, v. 23, p. 1179–1185, doi: 10.1016/S0191-8141(00)00185-1.

Lavier, L.L., Buck, W.R., and Poliakov, A.N.B., 1999, Self-consistent rolling-hinge model for the evolution of large-offset low-angle normal faults: Geology, v. 27, p. 1127–1130, doi: 10.1130/0091-7613(1999)027<1127:SCRHMF>2.3.CO;2.

McGrew, A.J., Peters, M.T., and Wright, J.E., 2000, Thermobarometric constraints on the tectonothermal evolution of the East Humboldt Range metamorphic core complex, Nevada: Geological Society of America Bulletin, v. 112, p. 45–60, doi: 10.1130/0016-7606(2000)112<0045:TCOTTE>2.3.CO;2.

Moresi, L., Dufour, F., and Mühlhaus, H.-B., 2003, A Lagrangian integration point finite element method for large deformation modeling of viscoelastic geomaterials: Journal of Computational Physics, v. 184, p. 476–497, doi: 10.1016/S0021-9991(02)00031-1.

Norlander, B.H., Whitney, D.L., Teyssier, C., and Vanderhaeghe, O., 2002, Partial melting and decompression of the Thor-Odin dome, Shuswap metamorphic core complex, Canadian Cordillera: Lithos, v. 61, p. 103–125, doi: 10.1016/S0024-4937(02)00075-0.

O'Neill, C., Moresi, L., Müller, D., Albert, R., and Dufour, F., 2006, Ellipsis 3D. A particle-in-cell finite-element hybrid code for modeling mantle convection and lithospheric deformation: Computers & Geosciences, v. 32, p. 1769–1779, doi: 10.1016/j.cageo.2006.04.006.

Regenauer-Lieb, K., Weinberg, R.F., and Rosenbaum, G., 2006, The effect of energy feedbacks on continental strength: Nature, v. 442, p. 67–70, doi: 10.1038/nature04868.

Rey, P., Vanderheaghe, O., and Teyssier, C., 2001, Gravitational collapse of continental crust: Definition, regimes, and modes: Tectonophysics, v. 342, p. 435–449, doi: 10.1016/S0040-1951(01)00174-3.

Richet, P., and Bottinga, Y., 1995, Rheology and configurational entropy of silicate melts, *in* Stebbens, J.F., et al., eds., Structure, dynamics and properties of silicate melts: Mineralogical Society of America Reviews in Mineralogy, v. 32, p. 67–93.

Rosenberg, C.L., and Handy, M.R., 2005, Experimental deformation of partially melted granite revisited: Implications for the continental crust: Journal of Metamorphic Geology, v. 23, p. 19–28, doi: 10.1111/j.1525-1314.2005.00555.x.

Scaillet, B., Holtz, F., Pichavant, M., and Schmidt, M., 1996, Viscosity of Himalayan leucogranites: Implications for mechanisms of granitic magma ascent: Journal of Geophysical Research, v. 101, no. B12, p. 27,691–27,700, doi: 10.1029/96JB01631.

Sullivan, W.A., and Snoke, A.W., 2007, Comparative anatomy of core-complex development in the northeastern Great Basin, U.S.A: Rocky Mountain Geology, v. 42, p. 1–29, doi: 10.2113/gsrocky.42.1.1.

Teyssier, C., and Whitney, D.L., 2002, Gneiss domes and orogeny: Geology, v. 30, p. 1139–1142, doi: 10.1130/0091-7613(2002)030<1139:GDAO>2.0.CO;2.

Teyssier, C., Ferré, E.C., Whitney, D.L., Norlander, B., Vanderhaeghe, O., and Parkinson, D., 2005, Flow of partially molten crust and origin of detachments during collapse of the Cordilleran orogen, *in* Bruhn, D., and Burlini, L., eds., High-strain zones: Structure and physical properties: Geological Society of London Special Publication 245, p. 39–64, doi: 10.1144/GSL.SP.2005.245.01.03.

Tirel, C., Brun, J.-P., and Burov, E., 2004, Thermomechanical modeling of extensional gneiss domes, *in* Whitney, D.L., et al., eds., Gneiss domes in orogeny: Geological Society of America Special Paper 380, p. 67–78.

Tirel, C., Brun, J.-P., and Burov, E., 2008, Dynamics and structural development of metamorphic core complexes: Journal of Geophysical Research, v. 113, B04403, doi: 10.1029/2005JB003694.

Vanderhaeghe, O., Teyssier, C., and Wysoczanski, R., 1999, Structural and geochronologic constraints on the role of partial melting during the formation of the Shuswap metamorphic core complex at the latitude of the Thor-Odin dome, British Columbia: Canadian Journal of Earth Sciences, v. 36, p. 917–943, doi: 10.1139/cjes-36-6-917.

Wdowinski, S., and Axen, G.J., 1992, Isostatic rebound due to tectonic denudation: A viscous flow model of a layered lithosphere: Tectonics, v. 11, p. 303–315, doi: 10.1029/91TC02341.

Whitney, D.L., Teyssier, C., and Fayon, A.K., 2004, Isothermal decompression, partial melting, and the exhumation of deep continental crust, *in* Grocott, J., et al., eds., Vertical coupling and decoupling in the lithosphere: Geological Society of London Special Publication 227, p. 313–326, doi: 10.1144/GSL.SP.2004.227.01.16.

Wijns, C., Weinberg, R., Gessner, K., and Moresi, L., 2005, Mode of crustal extension determined by rheological layering: Earth and Planetary Science Letters, v. 236, p. 120–134, doi: 10.1016/j.epsl.2005.05.030.

Wright, J.E., and Snoke, A.W., 1993, Tertiary magmatism and mylonitization in the Ruby–East Humboldt metamorphic core complex, northeastern Nevada: U-Pb geochronology and Sr, Nd, and Pb isotope geochemistry: Geological Society of America Bulletin, v. 105, p. 935–952, doi: 10.1130/0016-7606(1993)105<0935:TMAMIT>2.3.CO;2.

Manuscript received 20 August 2008
Revised manuscript received 5 December 2008
Manuscript accepted 8 December 2008

Printed in USA